

# Scaling properties of work fluctuations after quenches at quantum transitions

**Davide Nigro, Davide Rossini and Ettore Vicari**

Dipartimento di Fisica dell'Università di Pisa and INFN, Largo Pontecorvo 3, I-56127 Pisa, Italy

E-mail: `davide.rossini@unipi.it`

Authors are listed in alphabetic order

**Abstract.** We study the scaling properties of the statistics of the work done on a generic many-body system at a quantum phase transition of any order and type, arising from quenches of a driving control parameter. For this purpose we exploit a dynamic finite-size scaling framework. Namely, we put forward the existence of a nontrivial finite-size scaling limit for the work distribution, defined as the large-size limit when appropriate scaling variables are kept fixed. The corresponding scaling behaviors are thoroughly verified by means of analytical and numerical calculations in two paradigmatic many-body systems as the quantum Ising model and the Bose-Hubbard model.

*Keywords:* Finite-size scaling, Fluctuation phenomena, Quantum Phase Transitions, Quantum quenches

## 1. Introduction

Understanding the dynamics of quantum many-body systems is a highly non trivial task, which is nowadays gaining a great deal of interest, thanks to the amazing experimental progress in the field of quantum simulation. A paradigmatic setup is represented by ultracold atoms trapped in optical lattices: the system can be manipulated and controlled, both in space and in time, with an unprecedented accuracy as compared to any solid-state counterpart, preserving coherence over long time scales [1]. In the light of these achievements, it has become particularly relevant to develop specific theoretical frameworks that could work in out-of-equilibrium situations and for strong interactions, overcoming the limitations of linear-response and perturbation theory. The ultimate purpose is to shed light on some fundamental issues of quantum mechanics that have been recently resurfaced, such as equilibration and thermalization of closed systems [2, 3], or the emergence of universality in the dynamics across a critical point [4].

Important progress has been also made in the intimately related field of stochastic thermodynamics, where non-equilibrium fluctuation relations have been put forward,

both for classical [5, 6] and quantum [7, 8] systems. The beauty of fluctuation theorems stands on their completely general validity in out-of-equilibrium conditions, being able to characterize the full non-linear response of the system to any (perturbative or not) driving. These rely on the analysis of thermodynamic key concepts as work, heat, and entropy, which represent stochastic variables with definite probability distributions. We shall stress that, in the quantum realm, the notion of quantities such as the work performed on a system are not observables in the usual sense, but result from an out-of-equilibrium process [9, 10].

Here we focus on the statistics of the work done on a many-body system, close to a quantum phase transition, when this is driven out of equilibrium by suddenly switching one of the control parameters [7, 11]. Several issues related to this topic have been already discussed in a variety of physical implementations, including spin chains [12, 13, 14, 15, 16, 17, 18, 19], fermionic and bosonic systems [20, 21, 22, 23], quantum field theories [24, 25, 26, 27], as well as different contexts like cyclically driven systems [28] and dynamic quantum phase transitions [29]. It has been also shown that the work statistics can be experimentally measured in present-day ultracold-atom systems, by means of ion traps [30] or Ramsey interferometry [31, 32].

While the research done so far in this context has mostly addressed the thermodynamic limit of systems close to criticality (see, e.g., Ref. [11] and references therein), in order to achieve a deep understanding of any reliable quantum-simulation experiment, it is of primary importance to exploit the impact of having a finite size. Studying the finite-size dependence of the work statistics in nonequilibrium phenomena is also particularly attractive from a conceptual point of view. Indeed, for a global quench the work is extensive. Therefore in the thermodynamic limit, i.e., large-volume keeping the Hamiltonian parameter fixed, one expects the probability associated with the work density  $W/V$  (where  $V$  is the volume of the system) to be sharply peaked around its average value, with typical fluctuations suppressed as  $V^{-1/2}$ . This suggests that fluctuations around the work average, and in particular deviations from Gaussian behaviors, may be only observable for relatively small systems.

The natural theoretical context where to set up the analysis is the finite-size scaling (FSS) framework, that has been proven to be effective in proximity of any quantum transition. Indeed the emergence of FSS limits has been predicted both for continuous [33] and first-order [34] quantum transitions (CQTs and FOQTs, respectively), as well as in a dynamic FSS context (DFSS), to describe the quantum dynamics of finite-size many-body systems subject to time-dependent perturbations [35, 36]. Analogous FSS frameworks have been recently exploited to study quantum-information based concepts, as entanglement among parts of the system [37, 38, 33] as well as other indicators of genuine quantum correlations [39, 40, 41, 42, 43, 44], the fidelity [45, 46], and decoherence [47, 48, 49]. The purpose of this paper is to extend the analysis to the statistics of the work, and prove its validity in different paradigmatic quantum many-body systems, which exhibit both CQTs and FOQTs.

This paper is organized as follows. In Sec. 2 we fix our setting, by defining

the relevant quantities and the quench protocols that will be considered in the following. Section 3 contains our general DFSS framework for the work distribution, and constitutes the core of this work. We specifically address both continuous (Sec. 3.2) and first-order (Sec. 3.3) transitions, clarifying how the relevant scaling variables can be defined in the two cases. Our theory is then verified in the quantum Ising model (Sec. 4), both at its CQT and along the FOQT line, and in the hard-core Bose-Hubbard model (Sec. 5) across the vacuum-to-superfluid transition, also generalizing to the presence of an external trapping potential (Sec. 5.3). Finally, Sec. 6 is devoted to the conclusions and perspectives of this research.

## 2. Quench protocols and work fluctuations distribution

A sudden quench is a protocol which can be generally performed within a family of Hamiltonians, that are written as the sum of two noncommuting terms:

$$H(\lambda) = H_c + \lambda H_p. \quad (1)$$

The tunable parameter  $\lambda$  enables one to modify the strength of the *perturbation*  $H_p$ , e.g., a magnetic field term in a system of interacting spins, with respect to the *unperturbed* Hamiltonian  $H_c$ . We denote with  $|n_\lambda\rangle$  the eigenstates of energy  $E_n^\lambda$  of  $H(\lambda)$  (we assume a discrete spectrum, as it is generally appropriate for finite-size systems), in particular  $|0_\lambda\rangle$  is the corresponding ground state. The idea of a quantum quench is to prepare the system in the ground state of the Hamiltonian (1) for a given value  $\lambda_0$  of the  $\lambda$ -parameter, or in the corresponding equilibrium thermal state defined by the Gibbs distribution

$$p_n^{\lambda_0} = \frac{e^{-\beta E_n^{\lambda_0}}}{Z(\lambda_0)}, \quad Z(\lambda_0) = \sum_m e^{-\beta E_m^{\lambda_0}}. \quad (2)$$

Here  $\beta \equiv 1/T$  denotes the inverse temperature of a given heat reservoir, with which the system is initially coupled and in equilibrium (hereafter we will adopt units of  $\hbar = k_B = 1$ ). At time  $t = 0$ , the system-bath coupling is switched off and the  $\lambda$ -parameter is suddenly changed to  $\lambda \neq \lambda_0$ . One is then interested in studying the properties of the system, which unitarily evolves according to the post-quench Hamiltonian  $H(\lambda)$ , after a time  $t$ . In the case the initial condition is just the ground state  $|0_{\lambda_0}\rangle$  of  $H(\lambda_0)$ , or equivalently the zero-temperature limit of the Gibbs distribution, the resulting dynamic problem corresponds to that of the pure-state quantum evolution

$$|\Psi(t)\rangle = e^{-iH(\lambda)t}|0_{\lambda_0}\rangle, \quad (3)$$

with  $|\Psi(t=0)\rangle = |0_{\lambda_0}\rangle$  [2].

The quantum work  $W$  associated with such out-of-equilibrium dynamic protocol, i.e., the work done on the system by quenching the control parameter  $\lambda$ , does not generally have a definite value. More specifically, this quantity can be defined as the difference of two projective energy measurements [7]. The first one at  $t = 0$  projects

onto the eigenstates of the initial Hamiltonian  $H(\lambda_0)$  with a probability given by the equilibrium Gibbs distribution. Then the system evolves, driven by the unitary operator  $U(t, 0) = e^{-iH(\lambda)t}$ , and the second energy measurement projects onto the eigenstates of the Hamiltonian  $H(\lambda)$ . The work probability distribution can thus be written as [7, 10, 9]:

$$P(W) \equiv P(W, T, \lambda_0, \lambda) = \sum_{n,m} \delta[W - (E_n^\lambda - E_m^{\lambda_0})] |\langle n_\lambda | m_{\lambda_0} \rangle|^2 p_m^{\lambda_0}. \quad (4)$$

One may also introduce a corresponding characteristic function [12, 7]

$$C(s) = \int dW e^{isW} P(W), \quad (5)$$

encoding full information of the work statistics.

The work distribution (4) satisfies the quantum version of the Crooks fluctuation relation [7]

$$\frac{P(W, T, \lambda_0, \lambda)}{P(-W, T, \lambda, \lambda_0)} = e^{\beta W} e^{-\beta[F(\lambda) - F(\lambda_0)]}, \quad (6)$$

where the probability distribution in the denominator corresponds to an inverted quench protocol, from  $\lambda$  to  $\lambda_0$ . It also satisfies the Jarzynski equality [5, 7] [which can be directly derived from Eq. (6), as well]:

$$\langle e^{-\beta W} \rangle \equiv \int dW e^{-\beta W} P(W) = e^{-\beta[F(\lambda) - F(\lambda_0)]}, \quad (7)$$

where  $F(\lambda) = -T \ln Z(\lambda)$  is the free energy associated with the Hamiltonian parameter  $\lambda$ . Let us also define the so-called dissipative work [7]

$$W_i = W - [F(\lambda) - F(\lambda_0)], \quad (8)$$

satisfying the inequality  $\langle W_i \rangle \geq 0$ , which can be straightforwardly derived using Jensen's inequality.

The zero-temperature limit corresponds to a quench protocol from the ground state of  $H(\lambda_0)$ . Assuming that it is nondegenerate, the work probability (4) reduces to

$$P(W) = \sum_n \delta[W - (E_n^\lambda - E_0^{\lambda_0})] |\langle n_\lambda | 0_{\lambda_0} \rangle|^2, \quad (9)$$

and the dissipative work (8) simplifies to

$$W_i = W - (E_0^\lambda - E_0^{\lambda_0}). \quad (10)$$

In this case, the characteristic function  $C(s)$  can be simply written as the amplitude

$$C(s) = \langle 0_{\lambda_0} | e^{-iH(\lambda_0)s} e^{iH(\lambda)s} | 0_{\lambda_0} \rangle, \quad (11)$$

whose absolute value is related to the so-called Loschmidt echo  $Q(t) = -\ln |\langle 0_{\lambda_0} | \Psi(t) \rangle|^2$ , providing information on the overlap between the initial state  $|0_{\lambda_0}\rangle$  and the evolved quantum state  $|\Psi(t)\rangle$  at time  $t$ , cf. Eq. (3).

It is even possible to devise generalized time-dependent protocols, such as those starting from the ground state at  $\lambda_0$ , and then evolving the system by changing the protocol parameter  $\lambda_p(t)$  with a generic function of the time, up to a final value  $\lambda$ . In particular we may write it as

$$\lambda_p(t) = \lambda_0 + (\lambda - \lambda_0) f_p(t/t_p), \quad (12)$$

so that  $f_p(0) = 0$  and  $f_p(1) = 1$ , and  $t_p$  is the time scale of the variation. For example, one may consider a linear protocol  $f_p(x) = x$ . In this more general case, the work distribution (4) reads [7]:

$$P(W; f_p) = \sum_{n,m} \delta[W - (E_n^\lambda - E_m^{\lambda_0})] |\langle n_\lambda | U(t_p; f_p) | m_{\lambda_0} \rangle|^2 p_m^{\lambda_0}, \quad (13)$$

where  $U(t_p; f_p)$  is the evolution operator from  $t = 0$  to  $t_p$  associated with the time variation of Eq. (12). Of course, the general features of the dynamic behavior must somehow depend on the protocol function  $f_p(x)$ . In the limit  $t_p \rightarrow 0$ , we recover the sudden-quench protocol. Note also that, in the case of finite-size systems, even at quantum transitions, large time scales  $t_p$  must eventually give rise to quasi-static adiabatic evolutions, with vanishing dissipative work, i.e.,  $\langle W \rangle = F(\lambda) - F(\lambda_0)$ .

Let us finally comment on another out-of-equilibrium protocol based on a double sudden quench forming a cycle, similar to that discussed in Ref. [29]. The quantum evolution starts from an equilibrium Gibbs distribution at a given temperature  $T$ , associated with the Hamiltonian parameter  $\lambda_0$ . The  $\lambda$ -parameter is then suddenly changed to  $\lambda$ , at  $t = 0$ . After a time  $t$ , the parameter is suddenly quenched back to the value  $\lambda_0$ . The work distribution, associated with two projective energy measurements at  $t = 0$  and after the second quench at time  $t$ , can be written as

$$P(W) = \sum_{n,m} \delta[W - (E_n^{\lambda_0} - E_m^{\lambda_0})] |\langle n_{\lambda_0} | e^{-iH(\lambda)t} | m_{\lambda_0} \rangle|^2 p_m^{\lambda_0}. \quad (14)$$

Of course, in such case we have a further dependence on the time interval  $t$  in which the system evolves under the Hamiltonian  $H(\lambda)$ . The corresponding Jarzynski identity reads as  $\langle e^{-\beta W} \rangle = 1$ , since the double-quench protocol provides an out-of-equilibrium cycle returning to the initial value  $\lambda_0$  of the  $\lambda$ -parameter. The average work satisfies the thermodynamic inequality  $\langle W \rangle \geq 0$ , which can be easily derived using Jensen's inequality.

In the following sections we characterize the scaling behavior of the work fluctuations arising from the above quench protocols performed within the *critical* regime of a quantum transition. This requires that  $H_c$  describes a system either at a CQT or a FOQT, and that the temperature  $T$  is sufficiently low. Moreover, the perturbation  $\lambda H_p$ , driving the quench protocol, must be sufficiently small to maintain the system within the critical regime. In particular, we derive the scaling behaviors arising from the interplay of the temperature and the Hamiltonian parameters with the finite size  $L$  of the system. For this purpose, we are going to exploit an appropriate DFSS framework [35, 49].

### 3. Dynamic finite-size scaling of the work distribution

#### 3.1. General Ansatz

Let us start by considering a simple quench protocol, driven by the sudden change of the  $\lambda$ -parameter of the many-body Hamiltonian (1) at a quantum transition. We shall see that the DFSS framework allows us to study the interplay among the temperature  $T$ , the quench parameters  $\lambda_0$ ,  $\lambda$ , and the finite linear size  $L$ , assuming that the temperature is sufficiently small, and that both the initial ( $\lambda_0$ ) and final ( $\lambda$ ) parameters keep the system close to the transition point. The transition point is located at  $\lambda = 0$ , where the Hamiltonian is exactly  $H_c$ , while  $\lambda$  is a relevant parameter driving the transition.

Our working hypothesis is based on the existence of a nontrivial DFSS limit for the work distribution  $P(W)$ , defined as the large-size limit keeping the appropriate scaling variables fixed. Namely, we conjecture that, at both CQTs and FOQTs, the DFSS of the work distribution can be written as

$$P(W, T, \lambda_0, \lambda, L) \approx \Delta(L)^{-1} \mathcal{P}(\omega, \tau, \kappa_0, \kappa). \quad (15)$$

Here

$$\Delta(L) = \Delta(\lambda = 0, L), \quad (16)$$

where  $\Delta(\lambda, L)$  is the energy gap of the lowest states, while  $\mathcal{P}(\omega, \tau, \kappa_0, \kappa)$  is a function of the scaling variables

$$\omega = \Delta(L)^{-1} W, \quad \tau = \Delta(L)^{-1} T, \quad (17)$$

$\kappa_0$  and  $\kappa$ . The latter are other appropriate scaling variables proportional to  $\lambda_0$  and  $\lambda$ , respectively (see below). The DFSS limit is defined as the large-size  $L \rightarrow \infty$  limit, keeping the scaling variables  $\omega$ ,  $\tau$ ,  $\kappa_0$  and  $\kappa$  fixed.

The DFSS of the work distribution in Eq. (15) allows us to infer the scaling behavior of the average of the work and its higher moments, as well:

$$\langle W^k \rangle \equiv \int dW W^k P(W) \approx \Delta(L)^k \mathcal{W}_k(\tau, \kappa_0, \kappa), \quad (18)$$

with

$$\mathcal{W}_k(\tau, \kappa_0, \kappa) = \int d\omega \omega^k \mathcal{P}(\omega, \tau, \kappa_0, \kappa). \quad (19)$$

Of course  $\mathcal{W}_{k=0} = 1$ , corresponding to the normalization condition

$$\int dW P(W) = \int d\omega \mathcal{P}(\omega) = 1. \quad (20)$$

In the case of the work distribution (14) associated with a double quench protocol in which the  $\lambda$ -parameter is brought back to its initial value  $\lambda_0$  after a time  $t$ , we must add a further scaling variable

$$\theta_t = \Delta(L) t, \quad (21)$$

to take into account the dependence on the time interval of the evolution of the system under the Hamiltonian  $H(\lambda)$ . Scaling arguments analogous to those applied to the standard quench protocols [35] lead to the general DFSS ansatz

$$P(W, T, \lambda_0, \lambda, t, L) \approx \Delta(L)^{-1} \mathcal{P}(\omega, \tau, \kappa_0, \kappa, \theta_t), \quad (22)$$

at both CQTs and FOQTs.

As we shall see later, different scaling behaviors of the work distribution are expected to occur at CQTs and FOQTs, due to the different size dependence of the gap  $\Delta(L)$  and the FSS variables  $\kappa_0, \kappa$ : CQTs are generally characterized by power laws related to the universal critical exponent of the corresponding universality class, while exponential behaviors emerge at FOQTs. In the following we discuss more in detail the DFSS frameworks associated with CQTs and FOQTs, emphasizing their own peculiarities.

### 3.2. Continuous quantum transitions

The FSS theory at CQTs is well established (see, e.g., Refs. [33, 50, 51] and references therein). The energy differences  $\Delta_i(L) = E_i - E_0$  of the lowest states [and, in particular, of the ground-state gap  $\Delta(L) \equiv \Delta_1(L)$ ] at the transition point behave as

$$\Delta_i(L) \sim L^{-z}, \quad (23)$$

where  $z$  is a universal dynamic exponent. The FSS variable associated with the relevant scaling variable is

$$\kappa = L^{y_\lambda} \lambda, \quad (24)$$

where  $y_\lambda$  is a universal critical exponent, given by the renormalization-group (RG) dimension of the  $\lambda$  parameter. The equilibrium FSS limit of a generic observable  $O$ , obtained by taking  $L \rightarrow \infty$  keeping  $\kappa$  and  $\tau \sim L^z T$  fixed [see Eq. (17)], is expected to be

$$O(T, \lambda, L) \approx L^{-y_o} \mathcal{O}(\tau, \kappa), \quad (25)$$

where  $y_o$  is the RG dimension of the observable  $O$ , and  $\mathcal{O}$  is a universal FSS function depending on the geometry of the system and the type of boundary conditions.

Out-of-equilibrium time-dependent processes also require an appropriate rescaling of the time  $t$ , encoded by the scaling variable  $\theta_t \sim L^{-z} t$  [see Eq. (21)]. The corresponding DFSS limit is thus defined, in an analogous way, as the infinite-volume  $L \rightarrow \infty$  limit keeping the scaling variables  $\theta_t$ ,  $\tau$ ,  $\kappa$ , and  $\kappa_0 = L^{y_\lambda} \lambda_0$  fixed. Then a generic observable  $O$  in the DFSS limit is expected to behave as [35]

$$O(T, \lambda_0, \lambda, t, L) \approx L^{-y_o} \mathcal{O}(\tau, \kappa_0, \kappa, \theta_t), \quad (26)$$

where  $\mathcal{O}$  is a DFSS function.

The DFSS asymptotic behavior of the work probability distribution, given by Eq. (15), can be thus rewritten after defining a further scaling variable  $\omega \sim L^z W$  [see again Eq. (17)], such that

$$P(W, T, \lambda_0, \lambda, L) \approx L^z \mathcal{P}(\omega, \tau, \kappa_0, \kappa). \quad (27)$$

Correspondingly, its characteristic function  $C(s)$  is expected to behave as

$$C(s, T, \lambda_0, \lambda, L) \approx \mathcal{C}(\theta_s, \tau, \kappa_0, \kappa), \quad (28)$$

where  $\theta_s = \Delta(L) s \sim L^{-z} s$ , and

$$\mathcal{C}(\theta_s, \tau, \kappa_0, \kappa) = \int d\omega e^{i\theta_s \omega} \mathcal{P}(\omega, \tau, \kappa_0, \kappa). \quad (29)$$

Note that this DFSS is consistent with that expected for typical Loschmidt echos, along the quantum evolution after a quench protocol [35]. Indeed, due to Eq. (11), the variable  $s$  can be naturally considered as a time-like variable, explaining the time-like scaling of the corresponding FSS variable  $\theta_s$  [see Eq. (21)]. One may also derive nontrivial relations analogous to those of Eqs. (6) and (7) in terms of scaling functions and scaling variables only, using the scaling equation of the equilibrium free energy [33].

The approach to the asymptotic DFSS behavior is expected to be characterized by power-law suppressed corrections, typical of general CQTs [33]. In particular, we expect the existence of  $O(L^{-\omega})$  corrections, where  $\omega$  is the universal exponent associated with the leading irrelevant perturbation at the corresponding fixed point. Such corrections generally appear in the equilibrium critical behavior of correlations of local observables. The presence of boundaries generally gives rise to  $O(L^{-1})$  corrections, while in the absence of boundaries, like periodic boundary conditions, these corrections are absent. Moreover, for complex nonlocal quantities, such as the entanglement entropy between spatial regions, other peculiar power-law corrections may arise (see, e.g., Ref. [35] and references therein).

Using the general DFSS of the work probability, it is easy to derive the DFSS of the average work  $\langle W \rangle \approx \Delta(L) \mathcal{W}_1(\tau, \kappa_0, \kappa)$ . This becomes, in the zero-temperature limit,

$$\langle W \rangle \approx \Delta(L) \mathcal{W}_1(\kappa_0, \kappa). \quad (30)$$

We shall see here that the DFSS in Eq. (30) can be supported by an alternative derivation. The average work injected into the system by a quench from  $\lambda_0$  to  $\lambda$  is given by the expectation value of the post-quench Hamiltonian on the initial (pre-quench) state:

$$\langle W \rangle = \langle 0_{\lambda_0} | H(\lambda) - H(\lambda_0) | 0_{\lambda_0} \rangle = (\lambda - \lambda_0) \langle 0_{\lambda_0} | H_p | 0_{\lambda_0} \rangle. \quad (31)$$

It is easy to check that this equation corresponds to the integral  $\langle W \rangle = \int dW W P(W)$ , inserting  $P(W)$  as given in Eq. (9).



In the DFSS limit, we can exploit the equilibrium FSS behavior, cf. Eq. (25), to evaluate the matrix element  $\langle 0_{\lambda_0} | H_p | 0_{\lambda_0} \rangle$ . Assuming that  $H_p = \sum_{\mathbf{x}} P_{\mathbf{x}}$  is a sum of local terms, we have

$$\langle W \rangle \approx L^{d-y_p} (\lambda - \lambda_0) f_p(\kappa_0), \quad (32)$$

where  $y_p$  and  $f_p$  are, respectively, the RG dimension and the equilibrium FSS function associated with the observable  $H_p/L^d$  (here  $d$  is the dimensionality of the system). Taking into account the relation [52]

$$y_p + y_\lambda = d + z \quad (33)$$

between the RG dimensions of  $\lambda$  and of the associated perturbation  $H_p$ , Eq. (32) can be eventually written as

$$\langle W \rangle \approx L^{-z} (\kappa - \kappa_0) f_p(\kappa_0), \quad (34)$$

in agreement with Eq. (30), identifying

$$\mathcal{W}_1(\kappa_0, \kappa) \sim (\kappa - \kappa_0) f_p(\kappa_0). \quad (35)$$

This provides a relation between the DFSS function of the average work and the equilibrium FSS function of the expectation value of the Hamiltonian term  $H_p$  associated with the driving parameter  $\lambda$ .

We may also consider the large-volume limit of the above scaling behaviors. For  $L \rightarrow \infty$ , the average work is expected to grow as the volume, which implies

$$f_p(\kappa_0) \sim |\kappa_0|^{y_p/y_\lambda}, \quad |\kappa_0| \rightarrow \infty, \quad \langle W \rangle \sim L^d (\lambda - \lambda_0) |\lambda_0|^{y_p/y_\lambda}. \quad (36)$$

Note also that we may write it as

$$\frac{\langle W \rangle}{L^d} \sim \xi_0^{-(d+z)} \delta_\lambda, \quad (37)$$

where  $\xi_0 \sim |\lambda_0|^{-1/y_\lambda}$  represents an infinite-volume correlation length associated with the initial ground state of  $H(\lambda_0)$ , and  $\delta_\lambda = \lambda/\lambda_0 - 1 = \kappa/\kappa_0 - 1$ .

We stress that the DFSS relations derived above are quite general, in that they can be applied to any CQT, using the appropriate critical exponents associated with the corresponding universality class. Moreover, analogous considerations apply to local quenches, which can be described by a DFSS as well [36].

We finally mention that the work distribution in the infinite volume limit is expected to approach a quasi-Gaussian distribution around the average value of the work density  $W/L^d$  with  $O(L^{-d/2})$  fluctuations, which is expected to have the general form  $P(W) \sim \exp[-L^d I(W/L^d)]$  with  $I(x) \geq 0$  [21].

### 3.3. First-order quantum transitions

Let us now extend the above analysis to FOQTs. As shown by earlier works [34, 53, 54], isolated many-body systems at FOQTs develop FSS behaviors as well. However, they

significantly depend on the type of boundary conditions, in particular whether they favor one of the phases or they are neutral, giving rise to FSS characterized by exponential or power-law behaviors.

FOQTs generally arise from level crossings. However level crossings can only occur in the infinite-volume limit (in the absence of particular conservation laws). In a finite system, the presence of a nonvanishing matrix element among these states lifts the degeneracy, giving rise to the phenomenon of avoided level crossing. Here the FSS is controlled by the energy difference of the avoiding levels, in particular by the gap  $\Delta(L)$  of Eq. (16). The appropriate FSS variables are generally given by those in Eq. (17), and by [34]

$$\kappa = \Delta(L)^{-1} E_\lambda(\lambda, L), \quad (38)$$

$E_\lambda$  being the energy variation associated with the  $\lambda$  term (we assume  $E_\lambda = 0$  at the transition point). The DFSS limit is again defined by the large- $L$  limit, keeping  $\omega$ ,  $\tau$ , and  $\kappa$  fixed. Note that the FOQT scenario based on the avoided crossing of two levels is not realized for any boundary condition [34]: in some cases the energy difference  $\Delta(L)$  of the lowest levels may even show a power-law dependence on  $L$ . However, the scaling variables  $\kappa$  obtained using the corresponding  $\Delta(L)$  turn out to be appropriate as well [34].

Similarly to CQTs, the emergence of a DFSS after an out-of-equilibrium quench protocol  $\lambda_0 \rightarrow \lambda$  is also expected at FOQTs. The scaling arguments of Ref. [35] allow us to identify the additional variables  $\kappa_0 = \Delta(L)^{-1} E_\lambda(\lambda_0, L)$  and  $\theta_t = \Delta(L)t$  [see Eq. (21)]. Using arguments analogous to those at CQTs, we arrive at the DFSS of the work probability distribution given in Eq. (22). These considerations can be straightforwardly extended to generalized quench protocols, such as those introduced in Sec. 2.

The rest of the paper is dedicated to an explicit verification of the DFSS that we put forward for the work distribution after a quench in two paradigmatic examples of quantum many-body systems exhibiting transitions of different types and order. Namely, we focus on the quantum Ising model (Sec. 4) and on the Bose-Hubbard model (Sec. 5). We employ both numerical diagonalization techniques and analytical approaches, when possible.

## 4. Results for the quantum Ising model

### 4.1. The model

The Hamiltonian of the  $d$ -dimensional quantum Ising model defined on a lattice with  $L^d$  sites, in the presence of both a transverse and a longitudinal field, is given by:

$$H_{\text{Is}} = -J \sum_{\langle \mathbf{x}, \mathbf{y} \rangle} \sigma_{\mathbf{x}}^{(3)} \sigma_{\mathbf{y}}^{(3)} - g \sum_{\mathbf{x}} \sigma_{\mathbf{x}}^{(1)} - \lambda \sum_{\mathbf{x}} \sigma_{\mathbf{x}}^{(3)}. \quad (39)$$

Here  $\sigma^{(k)}$  denotes the spin-1/2 Pauli matrices ( $k = x, y, z$ ), the first sum is over all bonds connecting nearest-neighbor sites  $\langle \mathbf{x}, \mathbf{y} \rangle$ , while the other sums are over the sites. We

assume  $J = 1$  (ferromagnetic couplings) and  $g > 0$ . The phase diagram of these kinds of systems (in various dimensions) are known, and present both CQTs and FOQTs.

At  $g = g_c$  and  $\lambda = 0$  (in one dimension,  $g_c = 1$ ), the model undergoes a CQT belonging to the  $(d + 1)$ -dimensional Ising universality class [52, 55, 56], separating a disordered phase ( $g > g_c$ ) from an ordered ( $g < g_c$ ) one. The CQT at  $g = g_c$  is characterized by the presence of two relevant Hamiltonian parameters. They are  $r \equiv g - g_c$  and  $\lambda$  (such that they vanish at the critical point), with RG dimension  $y_r$  and  $y_\lambda$ , respectively. The equilibrium critical exponents  $y_r$  and  $y_\lambda$  are those of the  $(d + 1)$ -dimensional Ising universality class. For one-dimensional systems, they are  $y_r = 1/\nu = 1$  and  $y_\lambda = (d + 3 - \eta)/2 = (4 - \eta)/2$  with  $\eta = 1/4$ . For two-dimensional models, they are not known exactly, but there are very accurate estimates, see, e.g., Refs. [56, 57, 58, 59]; in particular [58]  $y_r = 1/\nu$  with  $\nu = 0.629971(4)$  and  $y_\lambda = (5 - \eta)/2$  with  $\eta = 0.036298(2)$ . For three-dimensional systems, they assume the mean-field values  $y_r = 2$  and  $y_\lambda = 3$ , apart from logarithms. The temperature  $T$  gives rise to a further relevant perturbation at CQTs; the corresponding scaling dimension is provided by the dynamic exponent  $z = 1$  (for any spatial dimension) characterizing the behavior of the energy differences of the lowest-energy states, and, in particular, the gap  $\Delta \sim \xi^{-z}$  where  $\xi$  is the diverging length scale at the transition point. Scaling corrections are generally controlled by the leading irrelevant perturbation, which gives rise to  $O(\xi^{-\omega})$  corrections to the asymptotic behavior, and the corresponding universal exponent is given by  $\omega = 2$  for  $d = 1$  [60] and  $\omega = 0.830(2)$  for  $d = 2$  [58].

For any  $g < g_c$ , the presence of a longitudinal external field  $\lambda$  drives FOQTs along the  $\lambda = 0$  line. The behavior along the FOQT line for  $g < g_c$  is related to the level crossing of the two lowest states  $|+\rangle$  and  $|-\rangle$  for  $\lambda = 0$ , such that  $\langle + | \sigma_{\mathbf{x}}^{(3)} | + \rangle = m_0$  and  $\langle - | \sigma_{\mathbf{x}}^{(3)} | - \rangle = -m_0$  (irrespective of  $\mathbf{x}$ ), with  $m_0 > 0$ . The degeneracy of these states is lifted by the longitudinal field  $\lambda$ . Therefore,  $\lambda = 0$  is a FOQT point, where the longitudinal magnetization  $M = L^{-d} \sum_{\mathbf{x}} M_{\mathbf{x}}$ , with  $M_{\mathbf{x}} \equiv \langle \sigma_{\mathbf{x}}^{(3)} \rangle$ , becomes discontinuous in the infinite-volume limit. The FOQT separates two different phases characterized by opposite values of the magnetization  $m_0$ , i.e.  $\lim_{\lambda \rightarrow 0^\pm} \lim_{L \rightarrow \infty} M = \pm m_0$ . For one-dimensional systems [61],  $m_0 = (1 - g^2)^{1/8}$ .

In a finite system of size  $L$ , the two lowest states are superpositions of two magnetized states  $|+\rangle$  and  $|-\rangle$ , in particular when the boundary conditions are neutral, i.e. they do not favor any of the two magnetized phases, such as periodic and open boundary conditions (see e.g. Refs. [34, 53, 54] for discussions of the scenario emerging when boundary conditions are not neutral). Due to tunneling effects, the energy gap  $\Delta$  at  $\lambda = 0$  vanishes exponentially as  $L$  increases, [62, 34]

$$\Delta(L) \sim e^{-cL^d}, \quad (40)$$

apart from powers of  $L$ . In particular, the energy gap  $\Delta(L)$  of the one-dimensional Ising ring (39) for  $g < 1$  is exponentially suppressed as [61, 63]

$$\Delta(L) = 2(1 - g^2)g^L [1 + O(g^{2L})] \quad (41a)$$

for open boundary conditions, and

$$\Delta(L) \approx 2 \sqrt{(1 - g^2)/(\pi L)} g^L \quad (41b)$$

for periodic boundary conditions. The differences for the higher excited states are finite, for  $L \rightarrow \infty$ .

In the following, we mostly consider quench protocols where the transverse field  $g$  is kept fixed, and  $\lambda$  is varied according to the various quench protocols described above. At  $g = g_c$ , the quench protocol provides a paradigmatic example of a CQT, while when  $g < g_c$  it provides examples of FOQTs.

#### 4.2. Work fluctuations at the continuous transition

We are now ready to present a numerical verification of the predicted DFSS behaviors for the work distribution associated with a quench of the one-dimensional quantum Ising model in the longitudinal field, at the continuous transition (see Sec. 3.2). In particular, we shall consider chains of size  $L$  with periodic boundary conditions, fix  $g = 1$  at the critical point, and study zero-temperature quench protocols driven by the longitudinal field,  $\lambda_0 \rightarrow \lambda$ , cf. Eq. (39).

Numerical diagonalization data concerning the scaling of the average post-quench work  $\langle W \rangle$ , defined in Eq. (31), are provided in Fig. 1, for a quench starting from  $\kappa_0 = 1$  and for different values of  $L$  up to 20 spins [64]. The average work is plotted against the post-quench renormalized field  $\kappa$ . We recall that, for the model under investigation, the RG dimension of the  $\lambda$  parameter is  $y_\lambda = 15/8$ , therefore Eq. (24) implies that  $\lambda = L^{-15/8} \kappa$  asymptotically approaches zero, in the large- $L$  limit (and analogously for  $\lambda_0$ ).

At a first glance, one realizes that data collapse emerges quite neatly already at very small sizes, on the scale of the figure. This obeys the scaling predicted by Eq. (30), after noticing that  $\Delta(L) \sim L^{-z}$ , and that  $z = 1$  for the one-dimensional quantum Ising ring. Therefore, the observed linear behavior of  $\langle W \rangle L$  as a function of  $\kappa$  (for fixed  $\kappa_0$ ) immediately follows from the scaling prediction, together with the identification of  $\mathcal{W}_1$  with that in Eq. (35). We have also analyzed finite-size corrections: the inset displays numerical data for a cut of the main frame at  $\kappa = -1.5$ . The approach to the asymptotic behavior appears to be characterized by  $O(L^{-2})$  corrections.

A closer inspection of higher moments of the work distribution is useful to test the scaling Ansatz put forward in Eq. (18). To this purpose, we have analyzed the numerical data for the second moment  $\langle W^2 \rangle$  of the work distribution, as well. Figure 2 displays the connected correlation function

$$\langle W^2 \rangle_c \equiv \langle W^2 \rangle - \langle W \rangle^2 \quad (42)$$

suitably rescaled by  $L^{2z} = L^2$ , as a function of the scaling variable  $\kappa$ , for the same set of parameters as in Fig. 1. Even in this case, we observe a remarkable agreement with the predicted DFSS behavior. We have checked that the predicted scaling occurs for several

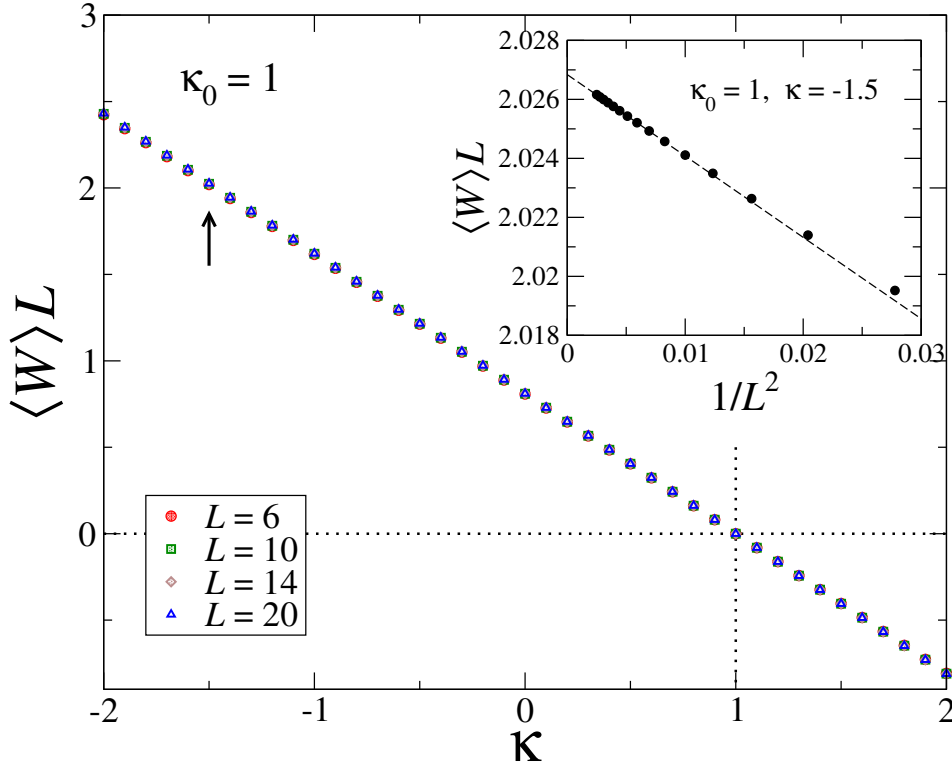


**Figure 1.** Average work  $\langle W \rangle$ , rescaled by a factor  $L^z = L$ , injected into the system after a quench of the Ising ring at the CQT, for fixed  $\kappa_0 = 1$  and varying  $\kappa$ . Notice that  $\kappa = \kappa_0$  corresponds to the equilibrium point, in which no work is performed on the system. The various data sets correspond to different chain lengths, as indicated in the legend. The inset shows the behavior of the same data with the system size, for fixed  $\kappa = -1.5$  (arrow in the main frame). The data appear to converge with  $O(L^{-2})$  corrections.

other choices of the system parameters, namely by varying  $\kappa_0$  and  $\kappa$  (not shown). The approach to the expected asymptotic behavior of the variance  $\langle W^2 \rangle_c$  turns out to be slower than the average work  $\langle W \rangle$ , as is visible in the inset (see the scale on the y-axis). Indeed, corrections appear to get suppressed as  $O(L^{-1})$ . This may suggest that the global convergence of the DFSS of the work statistics may be  $O(L^{-1})$ , similarly to the DFSS of the bipartite entanglement entropy [35]. We believe that this issue deserves further investigation.

It is significant to remark that the statistics of the work in the DFSS limit is generally not Gaussian, therefore higher moments of the work distribution are also important to be analyzed. In view of the fact that an increasing amount of computational resources is required to obtain  $\langle W^k \rangle$ , with  $k > 2$ , we decided to directly tackle the characteristic function of Eq (11) at finite times. To this purpose, instead of fully diagonalizing the post-quench Hamiltonian  $H(\lambda)$ , we have implemented the time evolution of the initial state  $|0_{\lambda_0}\rangle$  by means of a fourth-order Suzuki-Trotter decomposition of the unitary-evolution operator  $U(t) = e^{-iH(\lambda)t}$ , with a time step

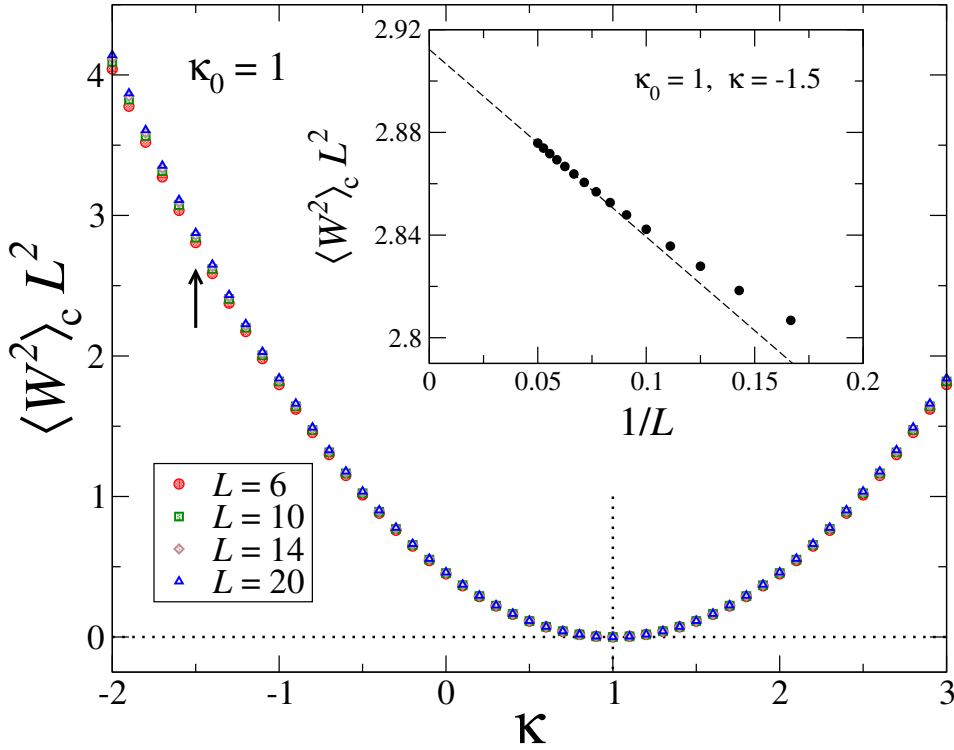


**Figure 2.** Same as in Fig. 1, but for the variance of the work distribution,  $\langle W^2 \rangle_c = \langle W^2 \rangle - \langle W \rangle^2$ , injected after the quench. The inset highlights the convergence to the asymptotic scaling behavior, which appears to follow a  $O(L^{-1})$  dependence. Unspecified parameters have been chosen to be the same as in Fig. 1.

$\delta t = 10^{-2}$ , for systems with up to  $L = 23$  sites.

We have eventually checked the DFSS prediction of Eq. (28), which entails the validity of the Ansatz for the whole distribution of the work statistics. The corresponding plot for the modulus of  $C(s)$ , as a function of the rescaled time variable  $\theta_s$ , is reported in Fig. 3 for three different values of  $\kappa_0$ , with  $\kappa = -\kappa_0$ . Even for this quantity, data collapse is remarkably evident at the relatively small sizes we were able to reach, with a slightly slower approach to the asymptotic scaling behavior when increasing  $\kappa$ . The convergence to the asymptotic DFSS behavior of  $C(s)$  appears consistent with a global  $s$ -dependent  $O(1/L)$  suppression of the corrections. Notice that the irregular pattern of the various curves signals the presence of non-Gaussian features in the statistics of the work. The irregularity of these curves, and thus the deviations from Gaussianity, is generally non monotonic in  $\kappa$ , since it depends on the degree of commensurability of the energy injected by the quench with the spectrum of the system [35].

Note that the main features of the DFSS at the CQT of the Ising models (39), such as the general size dependence and the scaling functions, are expected to be universal, i.e., they are expected not to depend on the microscopic details of the models (apart from trivial normalizations of the arguments). Therefore, their predictions can be extended

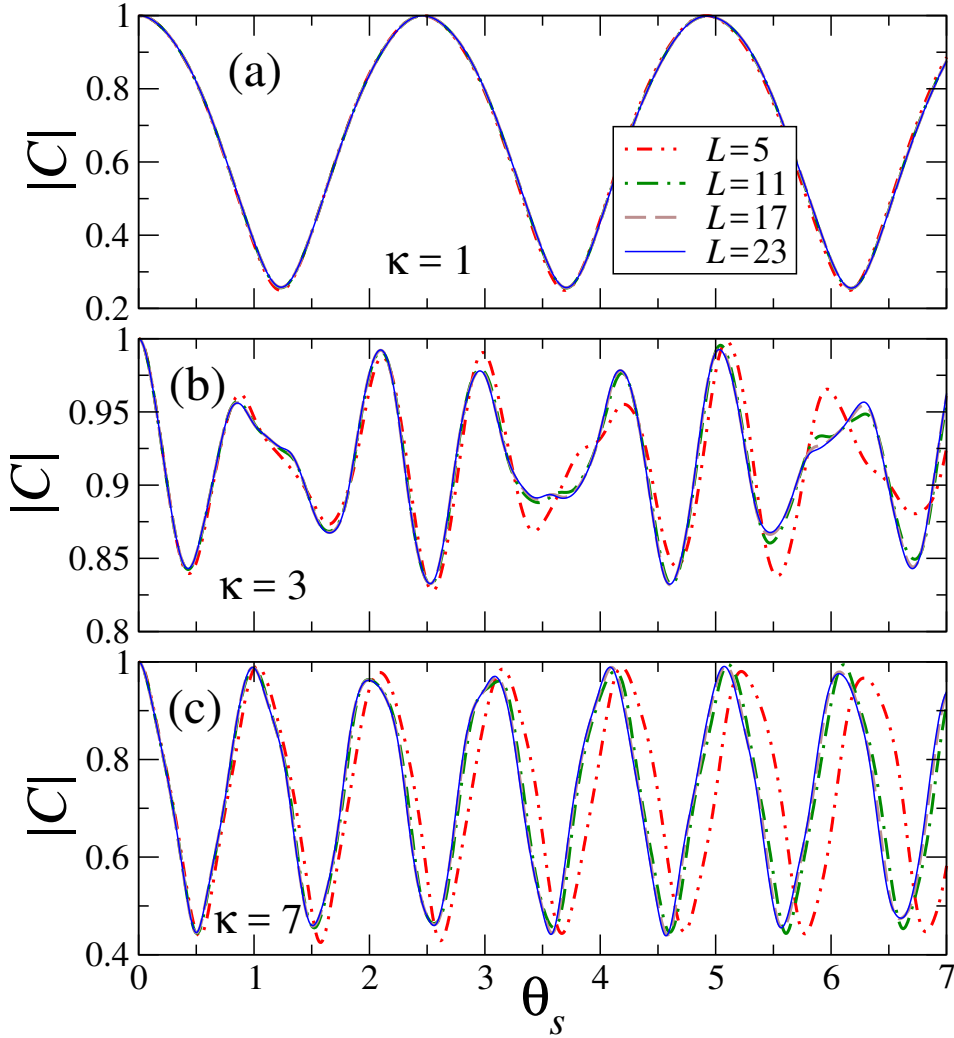


**Figure 3.** Scaling of the modulus of the characteristic function  $|C(s)|$  associated to a quench of the Ising model for  $\kappa = -\kappa_0$ . From top to bottom, the three panels refer to  $\kappa = 1, 3$ , and  $7$ , respectively. Data are plotted against the rescaled time  $\theta_s$ . Notice that, for the sake of convenience, in this figure we have defined  $\theta_s = L^z s$ , cf. Eq. (21).

to all CQTs belonging to the corresponding Ising universality classes.

#### 4.3. Work fluctuations at the first-order transitions

Let us now switch to the work distribution associated with quenches along the FOQT line of the model in Eq. (39), i.e., driven by the longitudinal external field  $\lambda$  along the line  $g < g_c$  of the phase diagram. As already mentioned, isolated many-body systems at FOQTs develop a FSS behavior, as well. However, they significantly depend on the type of boundary conditions, in particular whether they favor one of the phases or they are neutral, giving rise to FSS characterized by exponential or power-law behaviors. In the following we shall consider Ising systems with boundary conditions that do not favor any of the two magnetized phases, such as periodic and open boundary conditions,

which generally lead to exponential FSS laws [34]. We stress that, for peculiar boundary conditions as the antiperiodic ones, the energy difference of the lowest levels obeys a power-law dependence on  $L$ , in which case the situation becomes more subtle [34].

Following the general DFSS framework put forward in Sec. 3.3, we can identify the scaling parameters  $\kappa_0$ ,  $\kappa$ , and  $\theta_t$  (see Sec. 3.3). Specifically, as described in Sec. 4.2, we perform the quench protocol  $\lambda_0 \rightarrow \lambda$  for a value of  $g < g_c$ . The energy associated with the corresponding longitudinal-field perturbation  $\lambda$  is given by  $E_\lambda(\lambda, L) = 2m_0\lambda_0 L^d$ , while the gap  $\Delta(L)$  of the two lowest states at  $\lambda = 0$  is given by Eqs. (40), (41a), and (41b), depending on the boundary conditions. We can thus express the scaling variables  $\kappa_0$  and  $\kappa$  as [35]

$$\kappa_0 = \frac{2m_0\lambda_0 L^d}{\Delta(L)}, \quad \kappa = \frac{2m_0\lambda L^d}{\Delta(L)}. \quad (43)$$

The corresponding DFSS of the work distribution, Eq. (18), is expected to hold for any  $g < g_c$ , with a scaling function  $\mathcal{P}$  independent of  $g$ , apart from trivial normalizations of the arguments. The approach to the asymptotic scaling is expected to be exponential when increasing the size of the system (for the cases under consideration, the gap  $\Delta$  closes exponentially with  $L$ ).

In the case of the quantum Ising systems with periodic or open boundary conditions, the DFSS functions can be exactly computed, exploiting a two-level truncation of the spectrum [34, 36, 35]. In the long-time limit and for large systems, the scaling properties in a small interval around  $\lambda = 0$ , more precisely for  $m_0|\lambda| \ll \Delta_2 = O(1)$ , are captured by a two-level truncation, which only takes into account the two nearly degenerate lowest-energy states. The effective evolution is determined by the Schrödinger equation

$$i \frac{d}{dt} \Psi(t) = H_{2l}(\lambda) \Psi(t), \quad (44)$$

where  $\Psi(t)$  is a two-component wave function, whose components correspond to the states  $|+\rangle$  and  $|-\rangle$ , and

$$H_{2l}(\lambda) = -\beta \sigma^{(3)} + \delta \sigma^{(1)}, \quad \text{with } \beta = m_0\lambda L^d, \quad \delta = \Delta(L)/2. \quad (45)$$

Using Eq. (43), we also have  $\beta/\delta = \kappa$ . The initial condition is given by the ground state of  $H_{2l}(\lambda_0)$ :

$$|\Psi(\lambda_0, \lambda, L, t=0)\rangle = \sin(\alpha_0/2) |-\rangle - \cos(\alpha_0/2) |+\rangle, \quad (46)$$

with  $\tan \alpha_0 = \kappa_0^{-1}$  and  $\alpha_0 \in (0, \pi)$ . The quantum evolution after quenching  $\lambda_0 \rightarrow \lambda$  can be easily obtained by diagonalizing  $H_{2l}(\lambda)$ . Its eigenstates, associated with the eigenvectors  $E_{0,1}^\lambda = \mp \Delta \sqrt{1 + \kappa^2}/2$ , are

$$|0\rangle = \sin(\alpha/2) |-\rangle - \cos(\alpha/2) |+\rangle, \quad |1\rangle = \cos(\alpha/2) |-\rangle + \sin(\alpha/2) |+\rangle, \quad (47)$$

with  $\tan \alpha = \kappa^{-1}$  and  $\alpha \in (0, \pi)$ . Then, it is not difficult to show that, after the quench at  $t = 0$ , the state in Eq. (46) evolves as

$$|\Psi(\lambda_0, \lambda, L, t)\rangle = e^{i\frac{\theta_t}{2}\sqrt{1+\kappa^2}} \cos(\delta\alpha) |0\rangle + e^{-i\frac{\theta_t}{2}\sqrt{1+\kappa^2}} \sin(\delta\alpha) |1\rangle, \quad (48)$$



where we defined  $\delta\alpha = (\alpha_0 - \alpha)/2$ . Note that the time-dependent wave function in Eq. (48) is written in terms of scaling variables only.

Using these results, one can easily compute the characteristic function defined in Eq. (11), that is, the amplitude:

$$C(s) = e^{-iE_0 s} \langle \Psi(\lambda_0, \lambda, L, s = 0) | \Psi(\lambda_0, \lambda, L, -s) \rangle. \quad (49)$$

Therefore, the work probability distribution  $P(W)$  can be inferred directly from Eq. (5). Its corresponding scaling function [see Eq. (15)] reads:

$$\begin{aligned} \mathcal{P}^{(2l)}(\omega, \kappa_0, \kappa) &= \delta(\omega - \omega_-) \cos^2(\delta\alpha) + \delta(\omega - \omega_+) \sin^2(\delta\alpha), \\ \text{with } \omega_{\pm} &= \frac{1}{2} \left( \sqrt{1 + \kappa_0^2} \pm \sqrt{1 + \kappa^2} \right). \end{aligned} \quad (50)$$

This is in agreement with the expected scaling behavior.

Let us now specialize to the average work  $\langle W \rangle = \Delta(L) \mathcal{W}_1^{(2l)}(\kappa_0, \kappa)$ . After simple manipulations, working in the hypothesis of a two-level ( $2l$ ) truncation of the spectrum, this turns out to be characterized by the scaling function

$$\mathcal{W}_1^{(2l)}(\kappa_0, \kappa) = \frac{(\kappa_0 - \kappa)\kappa_0}{2\sqrt{1 + \kappa_0^2}}. \quad (51)$$

This expression has the same form of Eq. (35). It is instructive to see that it satisfies the inequality

$$\mathcal{W}_1^{(2l)} > \frac{1}{2} \left( \sqrt{1 + \kappa_0^2} - \sqrt{1 + \kappa^2} \right), \quad (52)$$

or, equivalently,

$$\langle W \rangle > E_0^\lambda - E_0^{\lambda_0}. \quad (53)$$

We remark that in the DFSS limit, the effects of higher states are expected to be exponentially suppressed, essentially because in this limit the probability associated with higher states is exponentially suppressed [36].

To corroborate the above DFSS predictions in the two-level truncation hypothesis close to a FOQT, we have numerically computed the average work after a quench in the longitudinal field  $\lambda$  for the one-dimensional quantum Ising chain at finite size  $L$ , with  $g < 1$ . The corresponding data for the ratio  $\langle W \rangle / \Delta(L)$ , at fixed  $g = 0.9$  and  $\kappa_0 = 1$ , are shown in Fig. 4 as a function of the rescaled variable  $\kappa$ . A comparison of the numerical outcomes with the analytic estimate  $\mathcal{W}_1^{(2l)}$  of Eq. (51) demonstrates a remarkable agreement between them, as is visible from the figure. A closer inspection to the behavior with  $L$ , for fixed  $\kappa$ , is provided in the inset, where an exponential convergence to the expected prediction clearly emerges. An analogous scaling behavior occurs for other values of  $g < 1$  (not shown), thus showing universality within the Ising-like FOQTs.

Let us close this discussion by mentioning that the above derived zero-temperature scaling formulas can be easily extended to finite temperature as well, using Eq. (4). This

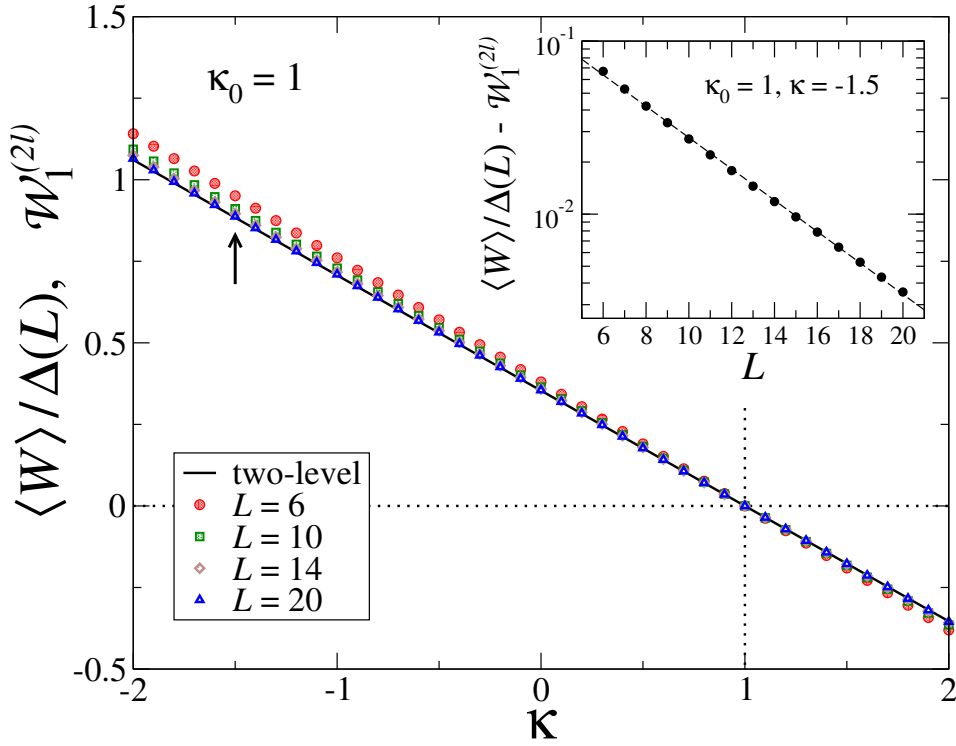


**Figure 4.** Average work  $\langle W \rangle$ , divided by the ground-state energy gap  $\Delta(L)$ , after a quench across the FOQT of the Ising ring with  $g = 0.9$  and  $\kappa_0 = 1$ , as a function of  $\kappa$  and for different chain lengths. The continuous straight line is the two-level prediction of Eq. (51). The inset highlights the difference between the numerical results at finite size and the analytic function  $\mathcal{W}_1^{(2l)}$ , which appears to decrease exponentially (the dashed line is an exponential fit of the data).

requires the further scaling variable  $\tau = \Delta(L)^{-1} T$ . The corresponding work distribution satisfies the Jarzynski equality, see Eq. (7):

$$\int dW e^{-\beta W} P(W, T, \lambda_0, \lambda, L) = e^{-\beta[F(\lambda) - F(\lambda_0)]}. \quad (54)$$

More precisely, using the fact that

$$P(W, T, \lambda_0, \lambda, L) = \Delta(L)^{-1} \mathcal{P}^{(2l)}(\omega, \tau, \kappa_0, \kappa), \quad (55)$$

cf. Eq. (15), we obtain

$$\int d\omega e^{-\omega/\tau} \mathcal{P}^{(2l)}(\omega, \tau, \kappa_0, \kappa) = \frac{\cosh[\sqrt{1 + \kappa^2}/(2\tau)]}{\cosh[\sqrt{1 + \kappa_0^2}/(2\tau)]}. \quad (56)$$

We finally address the quench protocol introduced at the end of Sec. 2. The quantum evolution starts from the ground state associated with the parameter value  $\lambda_0$ , which is suddenly changed to  $\lambda$  at  $t = 0$ . After a time  $t$  the parameter is quenched back to the value  $\lambda_0$ . In the case of FOQTs, two-level computations analogous to those

employed for the standard quench protocol confirm the conjectured scaling behaviors and allow us determine the corresponding scaling functions. We obtain

$$\mathcal{P}^{(2l)}(\omega, \kappa_0, \kappa, \theta_t) = A \delta(\omega) + (1 - A) \delta\left(\omega - \sqrt{1 + \kappa_0^2}\right), \quad (57)$$

where  $A \equiv |\langle 0_{\lambda_0} | \Psi(t) \rangle|^2$  denotes the overlap between the initial state and the time-evolved state, cf. Eq. (48), and is given by

$$A(\kappa_0, \kappa, \theta_t) = 1 - \frac{1}{2} \left[ 1 - \cos(\theta_t \sqrt{1 + \kappa^2}) \right] \sin^2(\alpha_0 - \alpha). \quad (58)$$

Finally, we would like to stress that the above DFSS of the work fluctuations is expected to be the same, apart from normalizations, along the FOQT line of the quantum Ising models (39) for  $g < g_c$ , and in any system sharing the same global properties, such as FOQTs arising from an avoided two-level crossing phenomenon in the large- $L$  limit.

## 5. Results for the Bose-Hubbard model

### 5.1. The lattice Bose-Hubbard model

Another physically interesting system is the Bose-Hubbard (BH) model [65], which provides a realistic description of a gas of bosonic atoms in an optical lattice [66]. Its Hamiltonian reads:

$$H_{\text{BH}} = -\frac{J}{2} \sum_{\langle \mathbf{x}, \mathbf{y} \rangle} (b_{\mathbf{x}}^\dagger b_{\mathbf{y}} + b_{\mathbf{y}}^\dagger b_{\mathbf{x}}) + \frac{U}{2} \sum_{\mathbf{x}} n_{\mathbf{x}}(n_{\mathbf{x}} - 1) - \mu \sum_{\mathbf{x}} n_{\mathbf{x}}, \quad (59)$$

where  $b_{\mathbf{x}}$  annihilates a boson on site  $\mathbf{x}$  of a cubic  $L^d$  lattice,  $n_{\mathbf{x}} \equiv b_{\mathbf{x}}^\dagger b_{\mathbf{x}}$  is the particle density operator, the first sum runs over the nearest-neighbor bonds  $\langle \mathbf{x}, \mathbf{y} \rangle$ , while the others run over the sites. Moreover the parameter  $J$  denotes the hopping strength,  $U$  the interaction strength, and  $\mu$  the onsite chemical potential. In addition, we consider a perturbation coupled to the particle operator  $b_{\mathbf{x}}$ , i.e.,

$$H(\lambda) = H_{\text{BH}} + \lambda H_p, \quad H_p = -\frac{1}{2} \sum_{\mathbf{x}} (b_{\mathbf{x}} + b_{\mathbf{x}}^\dagger), \quad (60)$$

where the parameter  $\lambda$  plays the role of a real external constant field. We express lengths in terms of the lattice spacing  $a = 1$  and set  $J = 1$ , so that energies are provided in units of  $J$ .

Here we are interested in the infinitely repulsive, hard-core  $U \rightarrow +\infty$  limit, so that the particle number can only take the values  $n_{\mathbf{x}} = 0, 1$ . In this case, the BH Hamiltonian  $H(\lambda) = H_{\text{BH}} + \lambda H_p$ , cf. Eq. (60), can be exactly mapped into the so-called XX model [52]

$$H_{\text{XX}} = - \sum_{\langle \mathbf{x}, \mathbf{y} \rangle} [S_{\mathbf{x}}^{(1)} S_{\mathbf{y}}^{(1)} + S_{\mathbf{x}}^{(2)} S_{\mathbf{y}}^{(2)}] + \mu \sum_{\mathbf{x}} \left( S_{\mathbf{x}}^{(3)} - \frac{1}{2} \right) - \lambda \sum_{\mathbf{x}} S_{\mathbf{x}}^{(1)}, \quad (61)$$

where the spin operators  $S_{\mathbf{x}}^{(k)} = \sigma_{\mathbf{x}}^{(k)}/2$  are related to the bosonic ones by:  $\sigma_{\mathbf{x}}^{(1)} = b_{\mathbf{x}}^{\dagger} + b_{\mathbf{x}}$ ,  $\sigma_{\mathbf{x}}^{(2)} = i(b_{\mathbf{x}}^{\dagger} - b_{\mathbf{x}})$ , and  $\sigma_{\mathbf{x}}^{(3)} = 1 - 2b_{\mathbf{x}}^{\dagger}b_{\mathbf{x}}$ .

The zero-temperature limit of the hard-core BH model, or equivalently of the XX model, displays three phases for  $\lambda = 0$ , associated with the ground-state properties [52]: the vacuum ( $\mu < -d$ ), the superfluid ( $-d < \mu < d$ ), and the Mott  $n = 1$  phase ( $\mu > d$ ). The vacuum-to-superfluid transition at  $\mu_{\text{vs}} = -d$  and the  $n = 1$  superfluid-to-Mott transition at  $\mu_{\text{sm}} = d$ , when they are driven by the chemical potential, belong to the universality class associated with a *nonrelativistic*  $U(1)$ -symmetric bosonic field theory [65]. The upper critical dimension of this bosonic field theory is  $d = 2$ . Thus its critical behavior is mean field for  $d > 2$ . For  $d = 2$  the field theory is essentially free (apart from logarithmic corrections), thus the dynamic critical exponent is  $z = 2$ , the RG dimension of the coupling  $\mu$  is  $y_{\mu} = 2$ . In  $d = 1$  the theory turns out to be equivalent to a free-field theory of nonrelativistic spinless fermions [52], from which one infers the RG exponents  $z = 2$  and  $y_{\mu} = 2$ . The RG dimension of the  $\lambda$  parameter of the Hamiltonians (60) and (61) is  $y_{\lambda} = z + d/2 = 2 + d/2$  (thus  $y_{\lambda} = 5/2$  for  $d = 1$ , and  $y_{\lambda} = 3$  for  $d = 2$ ).

### 5.2. Work fluctuations in quenches at the vacuum-to-superfluid transition

Let us concentrate on quench protocols at the vacuum-to-superfluid transition of the hard-core BH model (60), driven by the Hamiltonian variable  $\lambda$ , around the critical point  $\mu_{\text{vs}} = -d$  and  $\lambda = 0$ . According to the general DFSS theory outlined in Sec. 3, in particular Sec. 3.2, we expect the scaling behavior for the work distribution reported in Eq. (27), with  $z = 2$  and  $y_{\lambda} = 2 + d/2$ .

We have numerically checked these predictions by diagonalizing the XX chain with periodic boundary conditions [64]. The quench protocol  $\lambda_0 \rightarrow \lambda$  is performed at zero temperature, keeping  $\mu = \mu_{\text{vs}} = -1$  fixed. Data for the scaling of the average work  $\langle W \rangle$  at a given value of  $\kappa_0$  and for varying  $\kappa$  are presented in Fig. 5. Analogously to the continuous transition in the quantum Ising chain, reported in Fig. 1, we immediately realize that the data nicely collapse already for small sizes, exhibiting a linear behavior of  $\langle W \rangle L^z$  with  $z = 2$  as a function of  $\kappa$ ; this follows from the scaling prediction in Eqs. (30) and (35). The convergence to the asymptotic DFSS behavior is shown in the inset of Fig. 1.

The DFSS framework holds for all the moments of the work distribution. As a matter of fact, we have also analyzed in detail the connected correlator  $\langle W^2 \rangle_c$  and checked its scaling properties. Data collapse can be observed after a suitable rescaling, according to Eq. (18): pertinent data are presented in Fig. 6, where  $\langle W^2 \rangle_c L^{2z}$  is plotted against  $\kappa$ . Analogous results have been found for several other values of  $\kappa_0$  and  $\kappa$ .

Our results have been obtained in the hard-core  $U \rightarrow \infty$  limit. However, the DFSS behavior at the vacuum-to-superfluid transition is expected to be universal, thus independent of the on-site interaction strength  $U$ , apart from trivial normalizations (of course the location  $\mu_{\text{vs}}$  does depend on  $U$ ).

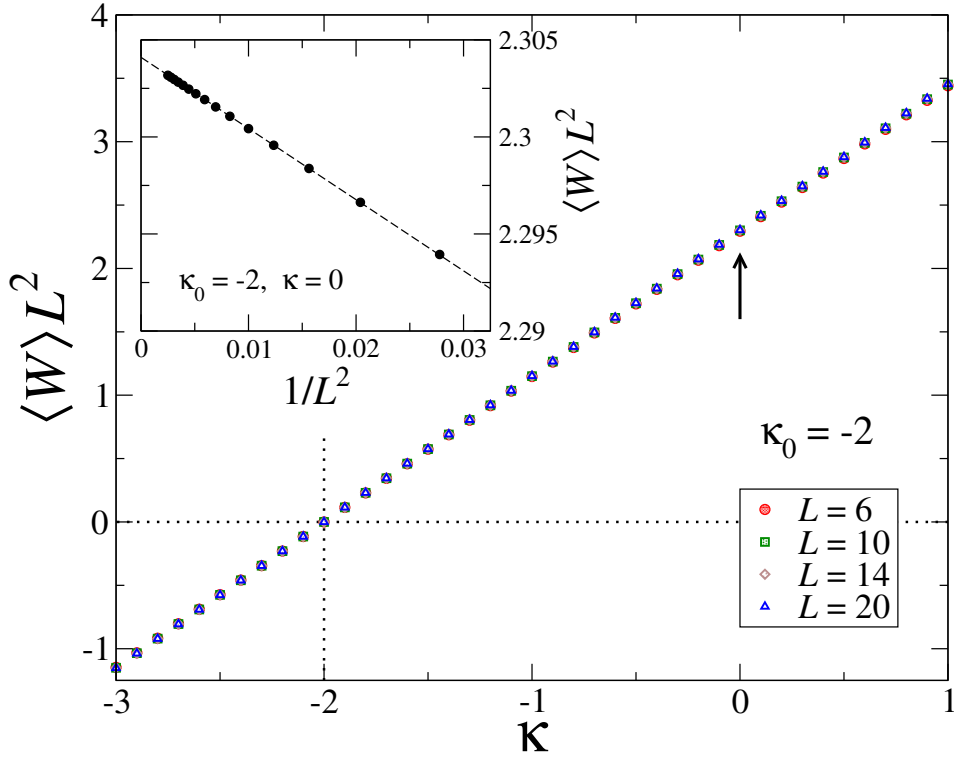


**Figure 5.** Average work  $\langle W \rangle$  for a quench of the XX model, rescaled by  $L^z = L^2$ , at fixed  $\kappa_0 = -2$  and for varying  $\kappa$ . The various data sets are for different chain lengths. The inset displays the behavior of the same data with the inverse square of the system size, for fixed  $\kappa = 0$  (arrow in the main frame). They appear to decrease as  $1/L^2$ .

We finally point out that one may also consider quench protocols driven by the Hamiltonian variable  $\mu$  around the critical point  $\mu = \mu_{\text{vs}}$  and  $\lambda = 0$ . In such case, unlike the quench protocol driven by the  $\lambda$  parameter, the driving Hamiltonian term commutes with the rest of the Hamiltonian. Dynamic scaling arguments apply as well. However, to keep this presentation self contained, we do not pursue this issue further.

### 5.3. Work fluctuations arising from variations of confining potentials

A common feature of any realistic experiment with cold atoms [1] is the presence of an external (typically harmonic) potential  $V(\mathbf{x})$  coupled to the particle density, which traps the particles within a limited space region. This section is devoted to a generalization of our DFSS considerations on the statistics of the work in the BH model, to the case in which the system is confined by a trapping potential.

Let us fix our setting by considering rotationally-invariant power-law potentials, of the form

$$V(\mathbf{x}, \ell) = v^p |\mathbf{x}|^p \equiv (|\mathbf{x}|/\ell)^p, \quad (62)$$

where  $v$  is the distance from the center of the trap, which we locate at the origin ( $\mathbf{x} = 0$ ) of the axis,  $p$  are positive constants and  $\ell \equiv 1/v$  is the trap size [67, 68]. Experiments

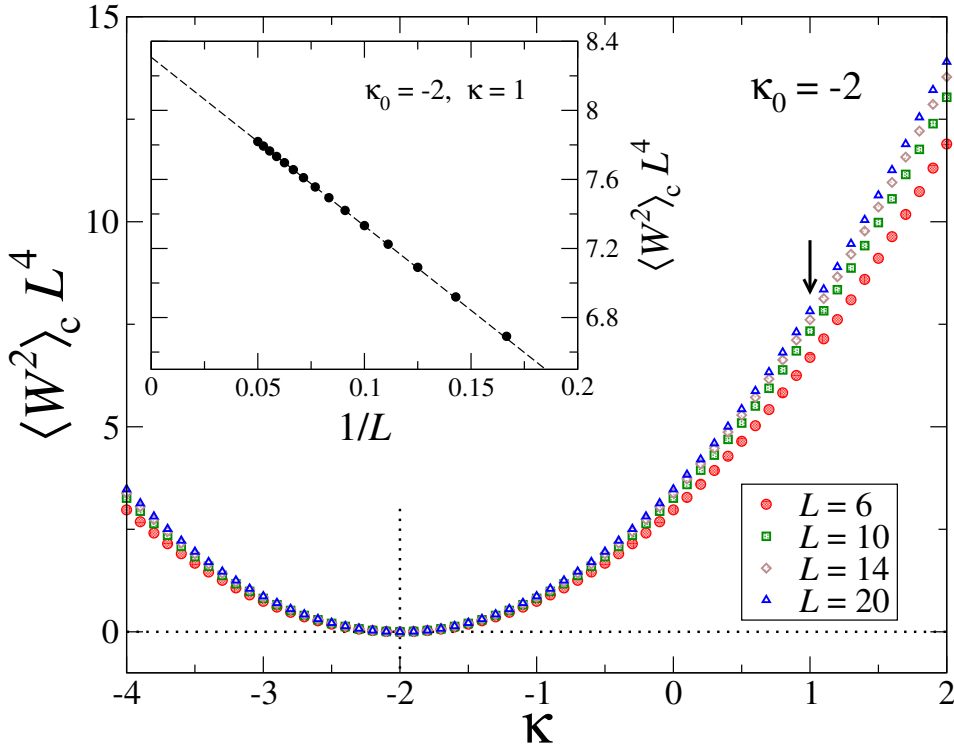


**Figure 6.** Same as in Fig. 5, but for the connected correlator  $\langle W^2 \rangle_c$ , rescaled by  $L^{2z} = L^4$ . In the inset we analyze the behavior with  $L$  at fixed  $\kappa = 1$  (arrow in the main frame), highlighting the convergence to the asymptotic behavior, which appears to be characterized by  $O(L^{-1})$  corrections, similarly to the results for the Ising chain at the critical point. Unspecified parameters have been chosen to be the same as in Fig. 5.

are usually set up with a harmonic potential, i.e.,  $p = 2$ . In the case of harmonic traps,  $\ell \sim \omega^{-1}$  where  $\omega$  is the trap frequency. This trapping force gives rise to a further inhomogeneous term to be added to the BH Hamiltonian (59), i.e,

$$H_{\text{tBH}} = H_{\text{BH}} + \sum_{\mathbf{x}} V(\mathbf{x}, \ell) n_{\mathbf{x}}. \quad (63)$$

Far from the origin, the potential  $V(\mathbf{x}, \ell)$  diverges, therefore  $\langle n_{\mathbf{x}} \rangle$  vanishes and the particles are trapped.

We want to infer the scaling properties of the work fluctuations at the vacuum-to-superfluid transition, arising from quench protocols varying the trap frequency, and therefore the trap size. Namely, we assume that the system is initially prepared in the ground state corresponding to the trap size  $\ell_0$ , and then the trap frequency is suddenly changed to a different value corresponding to a new trap size  $\ell$ , leading to a out-of-equilibrium quantum dynamics. Similar protocols have been discussed in Refs. [69, 70, 71].

The inhomogeneity due to the trapping potential strongly affects the phenomenology of quantum transitions in homogeneous systems. The trapping potential (62) cou-

pled to the particle density, as in Eq. (63), significantly affects the critical modes, introducing another *trap* length scale  $\ell$ . However, universal behaviors are recovered in the so-called trap-size scaling (TSS) limit [72]. The corresponding TSS behavior describes the distortion of the critical behavior around the center of the trap, due to the spatial inhomogeneity arising from the confining potential. TSS has some analogies with the FSS theory for homogeneous systems, with two main differences: the inhomogeneity induced by the space-dependence of the external field, and a nontrivial power-law dependence of the correlation length  $\xi_\ell$  when increasing the trap size  $\ell$  at the critical point, i.e.,

$$\xi_\ell \sim \ell^\theta, \quad (64)$$

where  $\theta$  denotes the universal *trap* exponent. The latter can be inferred by a RG analysis of the perturbation induced by the external trapping potential coupled to the particle density [72]. In the case of one-dimensional and two-dimensional BH models at their vacuum-to-superfluid and Mott transition driven by the chemical potential, the universal trap exponent is given by [67]

$$\theta = \frac{p}{p + y_\mu} = \frac{p}{p + 2}, \quad (65)$$

thus  $\theta = 1/2$  for harmonic confining potentials. Correspondingly, the gap at the transition points is expected to scale as [67]

$$\Delta(\ell) \sim \xi_\ell^{-z} \sim \ell^{-\theta z}, \quad (66)$$

where  $z = 2$  is the dynamic exponent associated with the transition of the homogeneous system, for both  $d = 1$  and  $d = 2$ . Within the TSS framework, the scaling law of the singular part of the free-energy density around the center of the trap is expected to behave as [67]

$$F(\mathbf{x}, \mu, T, \ell) \approx \xi_\ell^{-(d+z)} \mathcal{F}(\mathbf{x}_\ell, \mu_\ell, \tau_\ell), \quad (67)$$

$$\mathbf{x}_\ell = \mathbf{x}/\xi_\ell, \quad \mu_\ell = (\mu - \mu_{\text{vs}}) \xi_\ell^{y_\mu}, \quad \tau_\ell = T/\Delta(\ell). \quad (68)$$

Some issues concerning the equilibrium and out-of-equilibrium quantum coherence and entanglement properties of trapped gases have been already addressed [67, 73, 69, 74]. In particular, the study of the out-of-equilibrium quantum dynamics requires the introduction of a further scaling variable related to the time, i.e.

$$\theta_{t,\ell} = \Delta(\ell) t. \quad (69)$$

For example, when starting from the ground state of the initial trap, and suddenly changing its size from  $\ell_0$  to  $\ell$ , a generic observable is expected to develop a dynamic TSS behavior [69], such as

$$O(\mathbf{x}; \mu, \ell_0, \ell, t) \approx \xi_{\ell_0}^{-y_o} \mathcal{O}(\mathbf{x}_{\ell_0}, \mu_{\ell_0}, \theta_{t,\ell_0}, \delta_\ell), \quad (70)$$

$$\xi_{\ell_0} \sim \ell_0^\theta, \quad \theta_{t,\ell_0} = \Delta(\ell_0) t, \quad \delta_\ell = \frac{\ell - \ell_0}{\ell_0}, \quad (71)$$

where  $y_o$  is the RG exponent controlling the scaling behavior of the observable  $O$  at the vacuum-to-superfluid transition. The TSS limit is obtained by taking the arguments of the scaling function  $\mathcal{O}$  fixed. This dynamic TSS Ansatz has been confirmed by the time evolution of one-dimensional gases of impenetrable bosons [69].

In the following we discuss the scaling properties of the work fluctuations associated with quenches of the trap frequencies. The spectrum within a harmonic trap is discrete, thus the work fluctuation probability can be straightforwardly defined as in Eq. (9). The dynamic TSS is the optimal framework to infer the trap-size dependence of the work fluctuations after quenching the trap size. For this purpose, analogously to the case of the DFSS of homogeneous systems, we need to introduce a further scaling variable associated with the work variable  $W$ . We define

$$w_\ell = W/\Delta(\ell) \sim W \ell^{\theta_z}. \quad (72)$$

Using scaling arguments analogous to those exploited to investigate finite-size effects in homogeneous systems, we arrive at the TSS Ansatz

$$P(W, \mu, \ell_0, \ell) \approx \Delta(\ell_0) \mathcal{P}(w_{\ell_0}, \mu_{\ell_0}, \delta_\ell). \quad (73)$$

As a consequence, the dynamic TSS behavior of the average work reads:

$$\langle W \rangle \approx \Delta(\ell_0) \mathcal{W}_1(\mu_{\ell_0}, \delta_\ell). \quad (74)$$

The scaling behavior of the higher moments of the work fluctuations can be easily obtained from Eq. (73).

The dynamic TSS behavior of the work fluctuations can be checked by an alternative derivation of the scaling behavior (74) of the work average. Proceeding analogously to Sec. 3.2, we can write

$$\langle W \rangle = \langle 0_{\ell_0} | \sum_{\mathbf{x}} [V(\mathbf{x}, \ell) - V(\mathbf{x}, \ell_0)] n_{\mathbf{x}} | 0_{\ell_0} \rangle. \quad (75)$$

Then, using the TSS of particle density at the vacuum-to-superfluid transition [67],

$$\langle 0_{\ell_0} | n_{\mathbf{x}} | 0_{\ell_0} \rangle \approx \xi_{\ell_0}^{-(d+z-y_\mu)} \mathcal{D}(\mathbf{x}_\ell, \mu_\ell), \quad (76)$$

where  $\mathcal{D}$  is a TSS function, we easily recover the dynamic TSS reported in Eq. (74), with

$$\mathcal{W}_1(\mu_{\ell_0}, \delta_\ell) = -p \delta_\ell \int d^d \mathbf{x} |\mathbf{x}|^p \mathcal{D}(\mathbf{x}, \mu_{\ell_0}). \quad (77)$$

Analogous studies can be performed at the  $n = 1$  Mott transition. However, the corresponding dynamic behaviors is expected to be more complicated. We recall that the behavior around the  $n = 1$  Mott-to-superfluid transition of the homogeneous BH model without trap is essentially analogous to that at the vacuum-to-superfluid transition, because of the invariance under the particle-hole exchange. However, the particle-hole symmetry does not hold in the presence of the trapping potential, and the



asymptotic TSS dependence becomes more involved [67]. This is essentially related to the presence of level crossings at finite values of the trap size, where the gap vanishes. The resulting trap-size dependence can be cast in the form of a modulated TSS, that is a TSS controlled by the same exponents as those at the low-density vacuum-to-superfluid transition, but modulated by periodic functions of the trap size [67]. Analogous complications are expected to emerge also in dynamic behaviors arising from quench protocols. This issue however lies outside the purpose of the present work and is left for future investigations.

## 6. Summary and outlook

We have studied the scaling properties of the statistics of the work done on a many-body system after a quench in proximity of a quantum transition of any type. This has been done within a DFSS framework. Close to a quantum transition, an asymptotic DFSS behavior emerges from the interplay of the parameters involved in the quench protocol and the size of the system. In particular, we have considered a generic Hamiltonian  $H(\lambda) = H_c + \lambda H_p$ , with  $[H_c, H_p] \neq 0$ , and focused on a sudden change of the parameter  $\lambda$ , assuming that the pre- and post-quench Hamiltonians remain in the critical regime of a quantum transition. The DFSS limit is defined as the large-size limit keeping appropriate scaling variables fixed, associated with the Hamiltonian parameters, the temperature, etc. At CQTs these are ruled by suitable critical exponents and by the RG dimension of the tuning parameter, with typical power-law scaling behaviors. On the other hand, at FOQTs they are dictated by the size dependence of the energy gap, which is typically exponential, but can also be power-law, depending on the type of boundary conditions [34]. In our theoretical developments, we have also kept into account the effect of finite temperatures (for systems initially prepared into an equilibrium Gibbs ensemble), and discussed how it is possible to consider generalized time-dependent protocols.

We stress the generality of the scaling arguments that we used to develop the DFSS theory of the work fluctuations arising from quench at quantum transitions. As a consequence, they are expected to apply to generic CQTs and FOQTs in any spatial dimension. The DFSS framework allows us to infer the universal features of the scaling behaviors of the work fluctuations, such as their power laws and corresponding scaling functions (apart from trivial normalizations of the DFSS variables). Such predictions are expected to be independent of the microscopic details of the models at hand, but only determined by a few global properties shared by the universality class of the transition at CQTs, and by the general features of the FOQT, such as the fact that it may arise from a quasi-avoided two-level crossing in the large- $L$  limit.

The predictions of the DFSS theory have been verified in two paradigmatic quantum many-body systems, driven out of equilibrium by a time variation of one of their characterizing parameters: the quantum Ising and the Bose-Hubbard model. For the Ising model, we considered quenches associated with changes of a longitudinal

magnetic field. Depending on the value of the transverse field, the quench can drive the system through either CQTs or FOQTs. We explicitly tested our Ansatz by means of a numerical diagonalization of the Hamiltonian at CQTs in one dimension, and also through a two-level truncation of the spectrum at FOQTs. For the Bose-Hubbard model, we numerically studied quenches in the hard-core limit, driven by an external constant field globally coupled to the bosonic modes, through the vacuum-to-superfluid CQT. We also generalized the DFSS framework for the work fluctuations to describe particle systems confined by inhomogeneous external potentials; in particular, we considered quench protocols related to the variation of the size of the harmonic trap confining the particle gas.

Issues related to work fluctuations are particularly relevant for many-body systems of relatively small sizes, where they may be meaningful and also experimentally detectable, while they are conjectured to be largely suppressed in the thermodynamic limit. Indeed, in that case, sizable fluctuations of the intensive work density around its average value are expected to be extremely rare [21, 11], thus hardly observable. In this respect, approaches based on DFSS frameworks are particularly suitable to infer observable phenomena associated with quantum transitions in finite (even quite small) many-body systems, and capture their universal behaviors that are shared with a large class of models. Remarkably, our numerical results show that the DFSS behavior can be observed for relatively small sizes: in some cases a limited number of spins already displays the predicted asymptotic behavior. Therefore, even systems of modest size ( $L$  order of 10) may disclose the DFSS laws of the work fluctuations derived in this paper.

Given the actual experimental interest for the nonequilibrium aspects of the quantum dynamics of many-body systems, our results may be particularly relevant for experimental investigations of the properties of quantum work after quenches at quantum transitions. Present-day quantum-simulation platforms have already demonstrated their capability to reproduce and control the dynamics of quantum Ising-like chains with  $\sim 10$  spins. Ultracold atoms in optical lattices [75], trapped ions [76, 77, 78, 79, 80], and Rydberg atoms [81] may be promising candidates where the emerging universality properties of the quantum many-body physics can be tested with a minimal number of controllable objects.

## References

- [1] Bloch I, Dalibard J and Zwerger W, *Many-body physics with ultracold gases*, 2008 Rev. Mod. Phys. **80** 885
- [2] Polkovnikov A, Sengupta K, Silva A and Vengalattore M, *Colloquium: Nonequilibrium dynamics of closed interacting quantum systems* 2011 Rev. Mod. Phys. **83** 863
- [3] Nandkishore R and Huse D A, *Many body localization and thermalization in quantum statistical mechanics*, 2015 Annu. Rev. Condens. Matter Phys. **6** 15
- [4] Dziarmaga J, *Dynamics of a quantum phase transition and relaxation to a steady state*, 2010 Adv. Phys. **59** 1063
- [5] Jarzynski C, *Equalities and inequalities: Irreversibility and the second law of thermodynamics at the nanoscale*, 2011 Annu. Rev. Condens. Matter Phys. **2** 329

- [6] Seifert U, *Stochastic thermodynamics, fluctuation theorems and molecular machines*, 2012 Rep. Prog. Phys. **75** 126001
- [7] Campisi M, Hänggi P and Talkner P, *Colloquium: Quantum fluctuation relations: Foundations and applications*, 2011 Rev. Mod. Phys. **83** 771
- [8] Esposito M, Harbola U and Mukamel S, *Nonequilibrium fluctuations, fluctuation theorems, and counting statistics in quantum systems*, 2009 Rev. Mod. Phys. **81** 1665
- [9] Talkner P, Lutz E and Hänggi P, *Fluctuation theorems: Work is not an observable*, 2007 Phys. Rev. E **75** 050102(R)
- [10] Talkner P and Hänggi P, *Aspects of quantum work*, 2016 Phys. Rev. E **93** 022131
- [11] Goold J, Plastina F, Gambassi A and Silva A, *The role of quantum work statistics in many-body physics*, 2018 arXiv:1804.02805
- [12] Silva A, *Statistics of the Work Done on a Quantum Critical System by Quenching a Control Parameter*, 2008 Phys. Rev. Lett. **101** 120603
- [13] Dorosz S, Platini T and Karevski D, *Work fluctuations in quantum spin chains*, 2008 Phys. Rev. E **77** 051120
- [14] Dorner R, Goold J, Cormick C, Paternostro M and Vedral V, *Emergent Thermodynamics in a Quenched Quantum Many-Body System*, 2012 Phys. Rev. Lett. **109** 160601
- [15] Mascarenhas E, Braganc H, Dorner R, Franca Santos M, Vedral V, Modi K and Goold J, *Work and quantum phase transitions: Quantum latency*, 2014 Phys. Rev. E **89** 062103
- [16] Marino J and Silva A, *Non-Equilibrium Dynamics of a Noisy Quantum Ising Chain: statistics of the work and prethermalization after a sudden quench of the transverse field*, 2014 Phys. Rev. B **89** 024303
- [17] Zhong M and Tong P, *Work done and irreversible entropy production in a suddenly quenched quantum spin chain with asymmetrical excitation spectra*, 2015 Phys. Rev. E **91** 032137
- [18] Sharma S and Dutta A, *One- and two-dimensional quantum models: Quenches and the scaling of irreversible entropy*, 2015 Phys. Rev. E **92** 022108
- [19] Bayat A, Apollaro T J G, Paganelli S, De Chiara G, Johannessson H, Bose S and Sodano P, *Nonequilibrium critical scaling in quantum thermodynamics*, 2016 Phys. Rev. B **93** 201106(R)
- [20] Deffner S and Lutz E, *Nonequilibrium work distribution of a quantum harmonic oscillator*, 2008 Phys. Rev. E **77** 021128
- [21] Gambassi A and Silva A, *Large Deviations and Universality in Quantum Quenches*, 2012 Phys. Rev. Lett. **109** 250602
- [22] Shchadilova Y E, Ribeiro P and Haque M, *Quantum Quenches and Work Distributions in Ultralow-Density Systems*, 2014 Phys. Rev. Lett. **112** 070601
- [23] Sindona A, Goold J, Lo Gullo N and Plastina F, *Statistics of the work distribution for a quenched Fermi gas*, 2014 New J. Phys. **16** 045013
- [24] Sotiriadis S, Gambassi A and Silva A, *Statistics of the work done by splitting a one-dimensional quasicondensate*, 2013 Phys. Rev. E **87** 052129
- [25] Smacchia P and Silva A, *Work distribution and edge singularities for generic time-dependent protocols in extended systems*, 2013 Phys. Rev. E **88** 042109
- [26] Pálmai T and Sotiriadis S, *Quench echo and work statistics in integrable quantum field theories*, 2014 Phys. Rev. E **90** 052102
- [27] Pálmai T, *Edge exponents in work statistics out of equilibrium and dynamical phase transitions from scattering theory in one-dimensional gapped systems*, 2015 Phys. Rev. B **92** 235433
- [28] Bunin G, D'Alessio L, Kafri Y and Polkovnikov A, *Universal energy fluctuations in thermally isolated driven systems*, 2011 Nat. Phys. **7** 913
- [29] Heyl M, Polkovnikov A and Kehrein S, *Dynamical Quantum Phase Transitions in the Transverse-Field Ising Model*, 2013 Phys. Rev. Lett. **110** 135704
- [30] Huber G, Schmidt-Kaler F, Deffner S and Lutz E, *Employing trapped cold ions to verify the quantum Jarzynski equality*, 2008 Phys. Rev. Lett. **101** 070403
- [31] Dorner R, Clark S R, Heaney L, Fazio R, Goold J and Vedral V, *Extracting Quantum Work*

- Statistics and Fluctuation Theorems by Single-Qubit Interferometry*, 2013 Phys. Rev. Lett. **110** 230601
- [32] Mazzola L, De Chiara G and Paternostro M, *Measuring the characteristic function of the work distribution*, 2013 Phys. Rev. Lett. **110** 230602
  - [33] Campostrini M, Pelissetto A and Vicari E, *Finite-size scaling at quantum transitions*, 2014 Phys. Rev. B **89** 094516
  - [34] Campostrini M, Nespolo J, Pelissetto A and Vicari E, *Finite-size scaling at first-order quantum transitions*, 2014 Phys. Rev. Lett. **113** 070402; *Finite-size scaling at first-order quantum transitions of quantum Potts chains*, 2015 Phys. Rev. E **91** 052103
  - [35] Pelissetto A, Rossini D and Vicari E, *Dynamic finite-size scaling after a quench at quantum transitions*, 2018 Phys. Rev. E **97** 052148
  - [36] Pelissetto A, Rossini D and Vicari E, *Off-equilibrium dynamics driven by localized time-dependent perturbations at quantum phase transitions*, 2018 Phys. Rev. B **97** 094414
  - [37] Amico L, Fazio R, Osterloh A and Vedral V, *Entanglement in many-body systems*, 2008 Rev. Mod. Phys. **80** 517
  - [38] *Entanglement entropy in extended systems*, edited by Calabrese P, Cardy J and Doyon B, 2009 J. Phys. A **42** 500301
  - [39] Tomasello B, Rossini D, Hamma A and Amico L, *Ground-state factorization and correlations with broken symmetry*, 2011 Eur. Phys. Lett. **96** 27002
  - [40] De Chiara G, Lepori L, Lewenstein M and Sanpera A, *Entanglement spectrum, critical exponents, and order parameters in quantum spin chains*, 2012 Phys. Rev. Lett. **109** 237208
  - [41] Campbell S, Mazzola L, De Chiara G, Apollaro T J G, Plastina F, Busch Th. and Paternostro M, *Global quantum correlations in finite-size spin chains*, 2013 New J. Phys. **15** 043033
  - [42] Giampaolo S M and Hiesmayr B C, *Genuine multipartite entanglement in the XY model*, 2013 Phys. Rev. A **88** 052305
  - [43] Bayat A, *Scaling of tripartite entanglement at impurity quantum phase transitions*, 2017 Phys. Rev. Lett. **118** 036102
  - [44] De Chiara G and Sanpera A, *Genuine quantum correlations in quantum many-body systems: a review of recent progress*, 2018 Rep. Prog. Phys. **81** 074002
  - [45] Gu S-J, *Fidelity approach to quantum phase transitions*, 2010 Int. J. Mod. Phys. B **24** 437
  - [46] Rossini D and Vicari E, *Ground-state fidelity at first-order quantum transitions*, 2018 arXiv:1807.01674
  - [47] Zurek W H, *Decoherence, einselection, and the quantum origins of the classical*, 2003 Rev. Mod. Phys. **75** 715
  - [48] Jacquod Ph and Petitjean C, *Decoherence, entanglement and irreversibility in quantum dynamical systems with few degrees of freedom*, 2009 Adv. Phys. **58** 67
  - [49] Vicari E, *Decoherence dynamics of qubits coupled to systems at quantum transitions*, 2018 Phys. Rev. A **98** 052127
  - [50] Barber M N, *Finite-size scaling*, in *Phase transitions and critical phenomena*, vol. 8, page 145, Domb C and Lebowitz J L eds. (1983 Academic Press, London)
  - [51] *Finite Size Scaling and Numerical Simulations of Statistical Systems*, ed. Privman V (1990 World Scientific)
  - [52] Sachdev S, *Quantum Phase Transitions*, (1999 Cambridge University, Cambridge, England)
  - [53] Campostrini M, Pelissetto A and Vicari E, *Quantum transitions driven by one-bond defects in quantum Ising rings*, 2015 Phys. Rev. E **91** 042123; *Quantum Ising chains with boundary terms*, 2015 J. Stat. Mech. P11015.
  - [54] Pelissetto A, Rossini D and Vicari E, *Finite-size scaling at first-order quantum transitions when boundary conditions favor one of the two phases*, 2018 Phys. Rev. E **98** 032124
  - [55] Zinn-Justin J, *Quantum Field Theory and Critical Phenomena*, fourth edition (2002 Clarendon Press, Oxford)
  - [56] Pelissetto A and Vicari E, *Renormalization-group theory and critical phenomena*, 2002 Phys. Rep.

**368** 549

- [57] Hasenbusch M, *A finite size scaling study of lattice models in the three-dimensional Ising universality class*, 2010 Phys. Rev. B **82** 174433
- [58] Kos F, Poland D, Simmons-Duffin D and Vichi A, *Precision islands in the Ising and  $O(N)$  models*, 2016 J. High Energy Phys. **08** 036
- [59] Kompaniets M V and Panzer E, *Minimally subtracted six-loop renormalization of  $O(n)$ -symmetric  $\varphi^4$  theory and critical exponents*, 2017 Phys. Rev. D **96** 036016
- [60] Caselle M, Hasenbusch M, Pelissetto A and Vicari E, *Irrelevant operators in the two-dimensional Ising model*, 2002 J. Phys. A **35** 4861
- [61] Pfeuty P, *The one-dimensional Ising model with a transverse field*, 1970 Ann. Phys. **57** 79
- [62] Privman V and Fisher M E, *Finite-size effects at first-order transitions*, 1983 J. Stat. Phys. **33** 385
- [63] Cabrera G G and Jullien R, *Universality of Finite-Size Scaling: Role of the Boundary Conditions*, 1986 Phys. Rev. Lett. **57** 393; *Role of the boundary conditions in the finite-size Ising model*, 1987 Phys. Rev. B **35** 7062
- [64] For systems with up to  $L = 12$  sites, we used an exact diagonalization approach. For larger sizes, in order to evaluate the ground state  $|0_{\lambda_0}\rangle$  of the pre-quench Hamiltonian, we employed a Lanczos-like algorithm (note that the first and the second moment of the work distribution can be found without evaluating the full spectrum of the post-quench Hamiltonian). See: Lehoucq R, Sorensen D and Yang C, *ARPACK Users Guide: Solution of Large Scale Eigenvalue Problems by Implicitly Restarted Arnoldi Methods*, 1997 Rice Univ. Press, Houston, USA
- [65] Fisher M P A, Weichmann P B, Grinstein G and Fisher D S, *Boson localization and the superfluid-insulator transition*, 1989 Phys. Rev. B **40** 546
- [66] Jaksch D, Bruder C, Cirac J I, Gardiner C W and Zoller P, *Cold bosonic atoms in optical lattices*, 1998 Phys. Rev. Lett. **81** 3108
- [67] Campostrini M and Vicari E, *Quantum critical behavior and trap-size scaling of trapped bosons in a one-dimensional optical lattice*, 2010 Phys. Rev. A **81** 063614
- [68] Rigol M and Muramatsu A, *Universal properties of hard-core bosons confined on one-dimensional lattices*, 2004 Phys. Rev. A **70** 031603(R); *Ground-state properties of hard-core bosons confined on one-dimensional optical lattices*, 2005 Phys. Rev. A **72** 013604
- [69] Campostrini M and Vicari E, *Equilibrium and off-equilibrium trap-size scaling in 1D ultracold bosonic gases*, 2010 Phys. Rev. A **82** 063636
- [70] Vicari E, *Quantum dynamics and entanglement in one-dimensional Fermi gases released from a trap*, 2012 Phys. Rev. A **85** 062324
- [71] Collura M, Sotiriadis S and Calabrese P, *Equilibration of a Tonks-Girardeau gas following a trap release*, 2013 Phys. Rev. Lett. **110** 245301; *Quench dynamics of a Tonks-Girardeau gas released from a harmonic trap*, 2013 J. Stat. Mech. P09025
- [72] Campostrini M and Vicari E, *Critical behavior and scaling in trapped systems*, 2009 Phys. Rev. Lett. **102** 240601; 2009 Phys. Rev. Lett. (E) **103** 269901; *Trap-size scaling in confined particle systems at quantum transitions*, 2010 Phys. Rev. A **81** 023606
- [73] Campostrini M and Vicari E, *Bipartite quantum entanglement of one-dimensional lattice systems with a trapping potential*, 2010 J. Stat. Mech.: Theory Exp. P08020.
- [74] Calabrese P, Le Doussal P and Majumdar S N, *Random matrices and entanglement entropy of trapped Fermi gases*, 2015 Phys. Rev. A **91** 012303
- [75] Simon J, Bakr W S, Ma R, Tai M E, Preiss P M and Greiner M, *Quantum simulation of antiferromagnetic spin chains in an optical lattice*, 2011 Nature **472** 307
- [76] Edwards E E, Korenblit S, Kim K, Islam R, Chang M-S, Freericks J K, Lin G-D, Duan L-M and Monroe C, *Quantum simulation and phase diagram of the transverse-field Ising model with three atomic spins*, 2010 Phys. Rev. B **82** 060412(R)
- [77] Islam R, Edwards E E, Kim K, Korenblit S, Noh C, Carmichael H, Lin G-D, Duan L-M, Joseph Wang C-C, Freericks J K and Monroe C, *Onset of a quantum phase transition with a trapped*

- ion quantum simulator*, 2011 Nat. Commun. **2** 377
- [78] Lin G-D, Monroe C and Duan L-M, *Sharp Phase Transitions in a Small Frustrated Network of Trapped Ion Spins*, 2011 Phys. Rev. Lett. **106** 230402
- [79] Kim K, Korenblit S, Islam R, Edwards E E, Chang M-S, Noh C, Carmichael H, Lin G-D, Duan L-M, Joseph Wang C-C, Freericks J K and Monroe C, *Quantum simulation of the transverse Ising model with trapped ions*, 2011 New J. Phys. **13** 105003
- [80] Debnath S, Linke N M, Figgatt C, Landsman K A, Wright K and Monroe C, *Demonstration of a small programmable quantum computer with atomic qubits*, 2016 Nature **536** 63
- [81] Labuhn H, Barredo D, Ravets S, de Leseleuc S, Macri T, Lahaye T and Browaeys A, *Tunable two-dimensional arrays of single Rydberg atoms for realizing quantum Ising models*, 2016 Nature **534** 667